

## PHOTOACTIVE NANOCOMPOSITES OF ZINC OXIDE / CLAY TYPE

TOKARSKÝ Jonáš<sup>1,2</sup>, MAMULOVÁ KUTLÁKOVÁ Kateřina<sup>1</sup>

<sup>1</sup>Nanotechnology centre, VSB - Technical University of Ostrava, Ostrava, Czech Republic, EU

<sup>2</sup>IT4Innovations Centre of Excellence, VSB - Technical University of Ostrava, Ostrava, Czech Republic, EU

### Abstract

Photoactive nanomaterials are of considerable interest to the scientific community for many years and their importance increases with increasing environmental pollution. This study is focused on ZnO/clay photoactive nanocomposites where ZnO nanoparticles are the photoactive components and the clay serves as a cheap and chemically stable matrix on which the ZnO nanoparticles are anchored. Anchoring nanoparticles on the matrix is often used method allowing easier handling of the nanocomposite (clay particles are of micrometric sizes) in comparison with pure nanoparticles. Moreover, nanoparticles anchored on the matrix do not represent such an environmental and health risks (due to the reduced mobility) as pure nanoparticles. Two clays were used in this study: kaoline KKAF and Moroccan clay ghassoul, unique mixture of stevensite and sepiolite, from Jebel Ghassoul deposit in Morocco. Photoactive nanocomposites were prepared from ZnCl<sub>2</sub> and NaOH precursors using a simple hydrothermal method. Resulting samples were dried and calcined at 600 °C for 1 h. The precursors:clay ratios were chosen so that the nanocomposites contained 50 wt.% of ZnO. Nanocomposites were characterized using X-ray powder diffraction, UV-VIS diffuse reflectance spectroscopy, and scanning electron microscopy techniques. Photodegradation activities were evaluated by discoloration of acid orange 7 aqueous solutions under UV irradiation. Sizes of crystallites and band gap energies were determined. Mutual comparison of the properties of both nanocomposites and also the comparison with pure ZnO nanoparticles were carried out.

**Keywords:** Photodegradation activity, ZnO, clay, nanocomposite

### 1. INTRODUCTION

ZnO nanoparticles (NPs) exhibiting excellent photodegradation activity are widely studied and used nanomaterial. ZnO NPs are prepared using various precursors (ZnCl<sub>2</sub>+NaOH [1], Zn(NO<sub>3</sub>)<sub>2</sub>+NH<sub>3</sub> [2], Zn(Ac)<sub>2</sub>+LiOH [3], etc.) either in pure form [4,5] or anchored on suitable matrix [1,6,7,8]. Because of potential health and environmental risks of free ZnO NPs [9] the anchoring on solid crystalline matrix is very reasonable way how to obtain material in which the NPs retain their photoactivity and lose the mobility. In addition, matrix larger than NPs allows easier handling of resulting material. Clays are very suitable for this purpose, especially for their low cost, wide availability, chemical stability, and surface charge which facilitates anchoring of the NPs. Two clays were studied in this work. The first one, kaolin, is not used as often as other clays (mainly smectites) in composites of NP/clay type. The second one, Moroccan clay ghassoul, is used for the very first time as a matrix for NPs. Ghassoul [rasul] (GHA), unique mixture of stevensite and sepiolite, comes from the only known deposit in the world, Jbel Ghassoul in Morocco. In Maghreb and Middle-East it has been used for centuries as a natural soap but for other scientists than geologists remained unknown until the 20<sup>th</sup> century [10]. Only in the last decade GHA attracted interest of Moroccan, Spanish and French materials engineers. GHA was found to be very good adsorbent of metal and organic cations [11,12] and can be also used for the preparation of cordierite ceramics [13]. Nanotechnology centre in Ostrava is the first Czech scientific institute where the use of GHA as a matrix for NPs is studied. Present work is focused on the comparison of ZnO/KA and ZnO/GHA photoactive nanocomposites. X-ray powder diffraction, UV-VIS diffuse reflectance spectroscopy, and scanning electron microscopy techniques were used for the characterization. Sizes of crystallites and band gap energies were determined. Photodegradation activities of nanocomposites were evaluated by discoloration of Acid Orange 7 aqueous solutions under UV irradiation. Nanocomposites were compared each other and also with pure ZnO NPs.

## 2. MATERIALS AND METHODS

### 2.1. Preparation of the samples

ZnO NPs were prepared by mixing ZnCl<sub>2</sub> and NaOH (Lach-Ner, Czech Republic) aqueous solutions (molar ratio of Zn<sup>2+</sup>: OH<sup>-</sup> = 1:5) and stirring at 40 °C for 30 min. ZnO/KA and ZnO/GHA nanocomposites were prepared by addition of the solutions into the aqueous suspension of KA KKAF (LB MINERALS, Czech Republic) and GHA (Morocco), respectively, followed by stirring at 100 °C for 5 h. The precursors/clay ratio was chosen so that the nanocomposites contained 50 wt.% of ZnO. Resulting solid phase was washed with distilled water and dried at 105 °C for 24 h. According to our previous experience [14], one half of each sample was calcined at 600 °C for 1 h in order to increase the photoactivity. Dried and calcined samples are identified by numbers 1 (i.e., 105 °C) and 6 (i.e., 600 °C).

### 2.2. Characterization methods

X-ray powder diffraction (XRPD) patterns of all samples pressed in a rotational holder were recorded in reflection mode under CoK<sub>α</sub> irradiation ( $\lambda = 1.7889 \text{ \AA}$ ) using the Bruker D8 Advance diffractometer (Bruker AXS, Germany) equipped with a fast position sensitive detector VANTEC 1. Phase composition of the samples was evaluated using the ICDD PDF 2 Release 2014 database.

UV-VIS diffuse reflectance spectroscopy (DRS) was used for a qualitative description of the differences in the band gap shift. Samples were placed in a 5.0 mm quartz cell and the spectra were registered using spectrophotometer CINTRA 303 (GBC Scientific Equipment, Australia) equipped with a reflectance sphere. Band gap energies ( $E_g$ ) of the samples were evaluated using method described by Kočí et al. [15].

The morphology of samples was observed on a scanning electron microscope (SEM) Hitachi SU6600 (Hitachi Ltd., Japan) using SE (secondary electrons) mode. Accelerating voltage 5 kV was used. Elemental composition of the samples was determined using energy dispersive X-ray spectroscopy (EDS).

Photodegradation activity of the samples was evaluated by the discoloration of Acid Orange 7 (AO7) aqueous solution. In the first step, the suspension containing 0.05 g of the sample, 65 ml of demineralized water and 5 ml of the AO7 aqueous solution ( $c_0 = 6.259 \times 10^{-4} \text{ mol / dm}^3$ ) was stirred in the dark for 1 h in order to achieve the adsorption equilibrium. In the second step, the suspension was exposed to UV irradiation (UVP pen ray lamp, 365 nm) for 1 h. The extent of AO7 photodegradation was evaluated by the change in the intensity of absorption maximum of AO7 (480 nm) using CINTRA 303 UV-VIS spectrometer.

## 3. RESULTS AND DISCUSSION

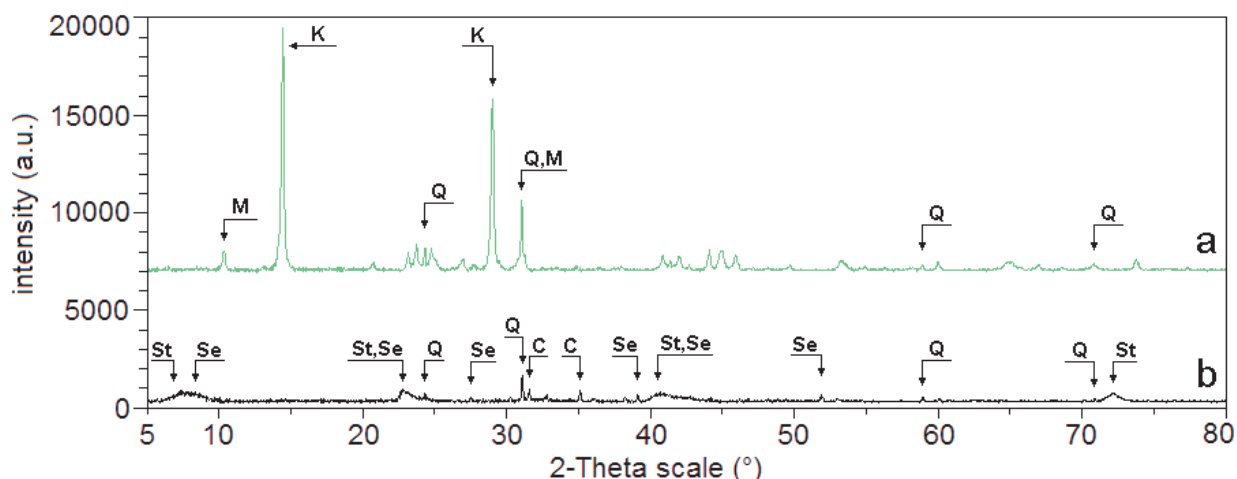


**Fig. 1** XRPD patterns of pure kaolin KKAF (a) and ghassoul (b) used for the preparation of nanocomposites. C - clinoenstatite, K - kaolinite, M - muscovite, Q - quartz, Se - sepiolite, St - stevensite

Composition of clays used for the preparation of nanocomposites was determined by XRPD analysis and the results are shown in **Fig. 1**. One can see that both clays contain admixtures. Dominant phase of KA, i.e., kaolinite ( $\text{Al}_4\text{Si}_4\text{O}_{10}(\text{OH})_8$ ; PDF number 75-1593), is accompanied by two other phases, muscovite ( $\text{Al}_3\text{Si}_3\text{O}_{10}(\text{OH},\text{F})_2$ ; PDF number 7-0042) and quartz ( $\text{SiO}_2$ ; PDF number 85-0798); see **Fig. 1a**. In case of kaolinite only two main, the most intensive reflections are marked. Remaining unmarked reflections in **Fig. 1a** belong also to kaolinite. Intensity of reflections in the XRPD pattern of GHA (**Fig. 1b**) is relatively low in comparison with KA suggesting lower crystallinity of this clay. Four phases - stevensite ( $\text{Mg}_3\text{Si}_4\text{O}_{10}(\text{OH})_2$ ; PDF number 25-1498), sepiolite ( $\text{Mg}_4\text{Si}_6\text{O}_{15}(\text{OH})_2$ ; PDF number 13-0595), clinoenstatite ( $\text{MgSiO}_3$ ; PDF number 84-0652), and quartz - were identified.

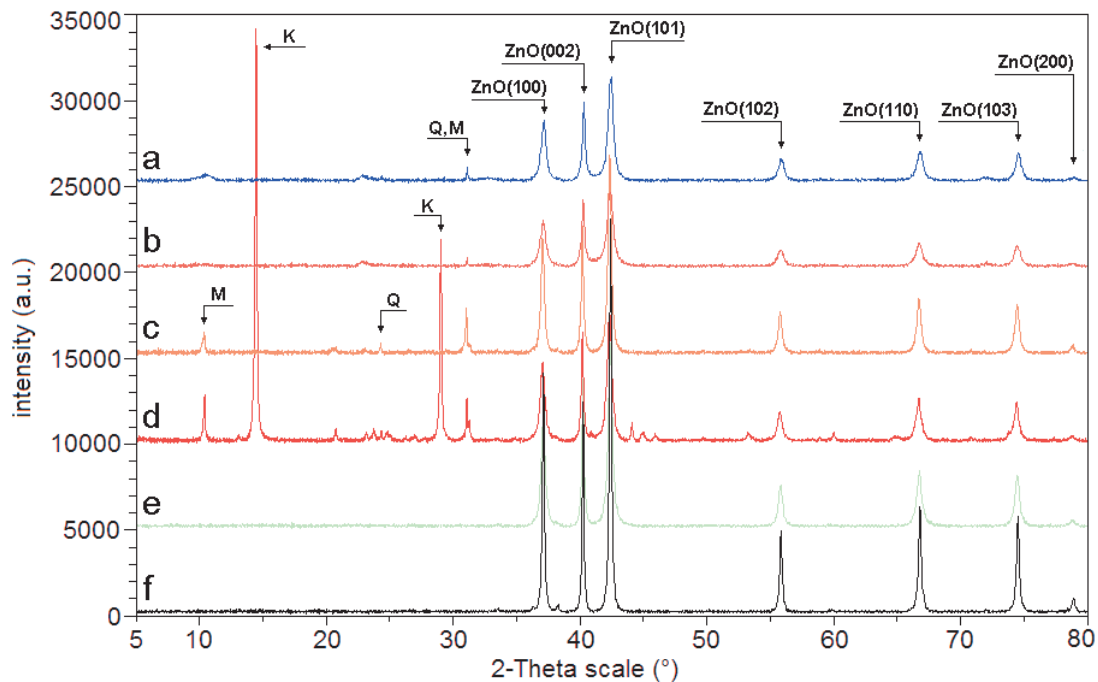


**Fig. 2** XRPD patterns of all prepared samples: (a) ZnO/GHA\_6, (b) ZnO/GHA\_1, (c) ZnO/KA\_6, (d) ZnO/GHA\_1, (e) ZnO\_1, (f) ZnO\_6. K - kaolinite, M - muscovite, Q - quartz

**Fig. 2** show XRPD patterns of all dried and calcined samples. Presence of ZnO (PDF number 70-2551) was confirmed in all of them and for individual ZnO reflections also Miller indices are presented. In all samples, ZnO has hexagonal (wurtzite) structure which is shown in **Fig. 3**. Dried and calcined samples of the same type are mutually not very different. The only significant difference can be found in case of ZnO/KA\_1 and ZnO/KA\_6 samples: after the calcination, diffraction peaks belonging to the kaolinite completely disappeared. This is caused by dehydroxylation of kaolinite sheets and subsequent phase transformation of crystalline kaolinite into amorphous metakaolinite at temperatures higher than  $\sim 450$  °C [16,17].

Calcined samples exhibit narrower and more intensive ZnO reflections. This can be attributed to better crystallinity and larger crystallite size of ZnO after the calcination. ZnO crystallite sizes ( $L_c$ ) were calculated according to the (101) ZnO diffraction peak ( $2\theta = 42.36$  °) using formula introduced by Scherrer [18]. Lanthanum hexaboride ( $\text{LaB}_6$ ) was used as a standard and calculated  $L_c$  values are listed in **Table 1**. While for ZnO/GHA composites the  $L_c$  values are smaller than for other samples, the  $L_c$  values for ZnO/KA and ZnO NPs are similar. **Table 1** shows that for all samples the calcination at 600 °C for 1 h led to higher

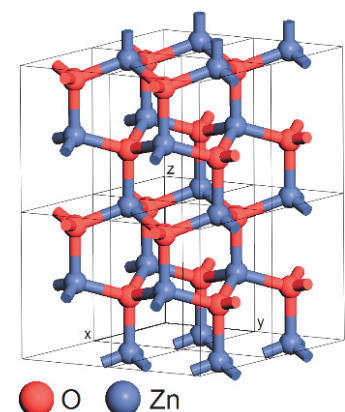


**Fig. 3** Hexagonal (wurtzite) structure of ZnO having lattice parameters:  $a = 3.24927$  Å,  $b = 3.24927$  Å,  $c = 5.20544$  Å,  $\alpha = 90$  °,  $\beta = 90$  °,  $\gamma = 120$  °

photodegradation activity. The most significant increase in photodegradation activity, more than 50 %, was observed in case of ZnO/KA composite. One can see that photodegradation activities of dried composites are lower than of dried ZnO NPs and after the calcination both ZnO/KA and ZnO/GHA composites exhibit higher photodegradation activity than calcined ZnO NPs. However, taking into account that composites contain only 50 wt.% ZnO, the photodegradation activity of composites is in fact significantly higher than of ZnO NPs even before the calcination. Anchoring of NPs on clay matrix prevents agglomeration of NPs and, therefore, larger surface of ZnO is available for the photodegradation process. KA was found to be more suitable matrix for ZnO NPs than GHA. Photodegradation activity of ZnO/KA\_6 sample reaches 95 % while in case of ZnO/GHA\_6 the photodegradation activity is 63 %. **Table 1** also shows that  $E_g$  values are lower for calcined composites than for calcined ZnO NPs. ZnO/KA\_6 sample exhibits the lowest  $E_g$  which is in good agreement with the highest photodegradation activity.

**Table 1** Photodegradation activity (PA), size of ZnO crystallites ( $L_c$ ) and band gap energy ( $E_g$ ) values for all prepared samples

samples	PA (%)	$L_c$ (nm)	$E_g$ (eV)
ZnO_1	56	26.7	3.20
ZnO_6	60	44.2	3.18
ZnO/KA_1	45	30.5	3.18
ZnO/KA_6	95	46.2	3.07
ZnO/GHA_1	42	20.8	3.25
ZnO/GHA_6	63	23.0	3.16

SEM images of ZnO/KA\_6 and ZnO/GHA\_6 composites show the morphology of the samples (**Fig. 4**). It can be clearly seen that ZnO has a “desert rose” crystal habit common for ZnO prepared from  $ZnCl_2$  [19]. Further it seems that ZnO NPs on GHA surface create rather separate islands, round and closed, while the areas of KA are covered by continuous layer. This could be one of the reasons causing the difference in PA.

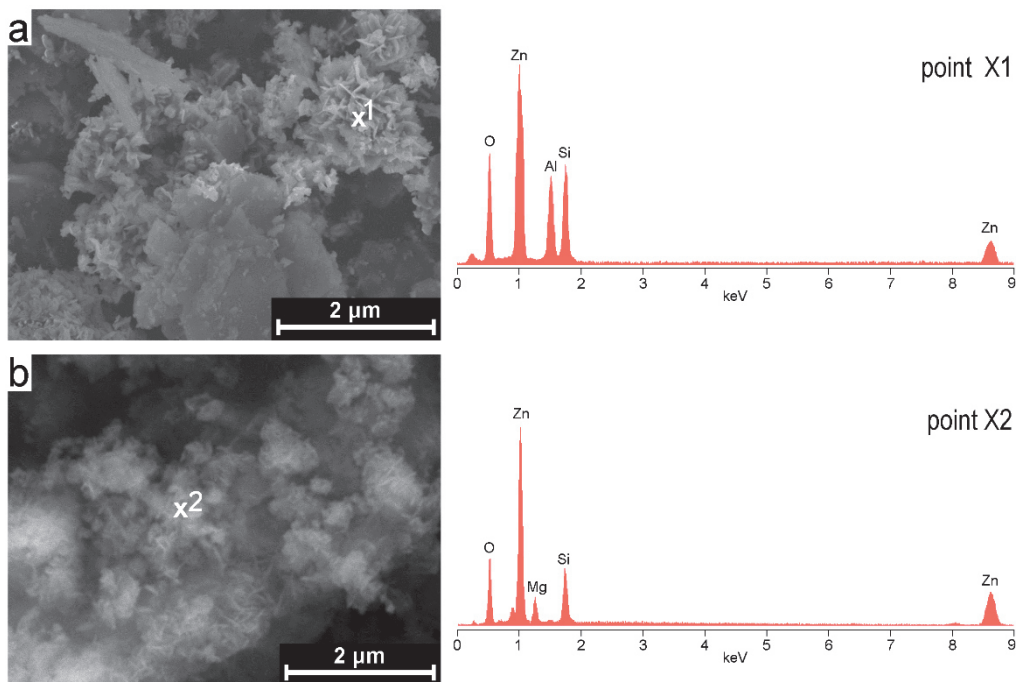


**Fig. 4** SEM images of (a) ZnO/KA\_6 composite, and (b) ZnO/GHA\_6 composite. EDS analysis of ZnO/KA\_6 (point X1) and ZnO/GHA\_6 (point X2) revealed chemical composition of the samples

EDS and XRPD results are in good agreement. Both analyses confirmed presence of ZnO in nanocomposites and revealed differences between used clays. Presence of Al in ZnO/KA\_6 sample corresponds with aluminosilicate phases in KA, while presence of Mg in ZnO/GHA\_6 sample corresponds with magnesiumsilicate phases in GHA (compare **Figs. 1 and 4**).

#### 4. CONCLUSIONS

Two clays, kaolin KKAF and ghassoul, mixture of stevensite and sepiolite, were studied as matrices for photoactive ZnO nanoparticles. It was found that ZnO/clay nanocomposites exhibit higher photodegradation activity than pure ZnO nanoparticles. Calcination at 600 °C for 1 h led to further increase in the photodegradation activity reaching 95 %, 63 %, and 60 % for ZnO/kaolin, ZnO/ghassoul, and pure ZnO nanoparticles, respectively. Taking into account that the same amount of pure ZnO nanoparticles and nanocomposites was used for the photodegradation experiments and that nanocomposites contain only 50 wt.% of ZnO, it can be concluded that these clay-based nanocomposites exhibit significantly higher photodegradation activity than pure ZnO nanoparticles. Silicate nature of clay matrices allows an easy use of the composites in building materials (mortars, plasters) but other applications, like wastewater treatment, can be also considered.

#### ACKNOWLEDGEMENTS

*This work was supported by the Ministry of Education, Youth and Sports of Czech Republic (project reg. no. SP2015/60) and by the European Regional Development Fund in the IT4Innovations Centre of Excellence (project reg.no. CZ.1.05/1.1.00/02.0070). Authors thank Vladimír Foldyna for the preparation of samples.*

#### REFERENCES

- [1] KHAORAPAPONG N., KHUMCHOO N., OGAWA M. Preparation of Zinc Oxide-Montmorillonite Hybrids, *Materials Letters*. Vol. 65, No. 4, 2011, pp. 657-660.
- [2] HUANG J., WU Y., GU C., ZHAI M., SUN Y., LIU J. Fabrication and Gas-Sensing Properties of Hierarchically Porous ZnO Architectures. *Sensors and Actuators B*, Vol. 155, No. 1, 2011, pp. 126-133.
- [3] COLLARD X., EL HAJJ M., SU B.-L., APRILE C. Synthesis of Novel Mesoporous ZnO/SiO<sub>2</sub> Composites for the Photodegradation of Organic Dyes, *Microporous and Mesoporous Materials*. Vol. 184, 2014, pp. 90-96.
- [4] SALEH R., DJAJA N.F. Transition-Metal-Doped ZnO Nanoparticles: Synthesis, Characterization and Photocatalytic Activity under UV Light. *Spectrochimica Acta A*, Vol. 130, 2014, pp. 581-590.
- [5] WANG H., XIE C. The Effects of Oxygen Partial Pressure on the Microstructures and Photocatalytic Property of ZnO Nanoparticles. *Physica E*, Vol. 40, No. 8, 2008, pp. 2724-2729.
- [6] LI S.Q., ZHOU P.J., ZHANG W.S., CHEN S., PENG H. Effective Photocatalytic Decolorization of Methylene Blue Utilizing ZnO/Rectorite Nanocomposite Under Simulated Solar Irradiation, *Journal of Alloys and Compounds*, Vol. 616, 2014, pp. 227-234.
- [7] FATIMAH I., WANG S., WULANDARI D. ZnO/Montmorillonite for Photocatalytic and Photochemical Degradation of Methylene Blue, *Applied Clay Science*, Vol. 53, No. 4, 2011, pp. 553-560.
- [8] LI X., YANG H. Pd Hybridizing ZnO/Kaolinite Nanocomposites: Synthesis, Microstructure, and Enhanced Photocatalytic Property. *Applied Clay Science*, Vol. 100, 2014, pp. 43-49.
- [9] MA H., WILLIAMS P.L., DIAMOND S.A. Ecotoxicity of Manufactured ZnO Nanoparticles: A Review. *Environmental Pollution*, Vol. 172, 2013, pp. 76-85.
- [10] CHAHI A., DURINGER P., AIS M., BOUABDELLI M., GAUTHIER-LAFAYE F., FRITZ B. Diagenetic Transformation of Dolomite into Stevensite in Lacustrine Sediments from Jbel Rhassoul, Morocco. *Journal of Sedimentary Research*, Vol. 69, No. 5, 1999, pp. 1123-1135.
- [11] EL MOUZDAHIR Y., ELMCHAOURI A., MAHBOUB R., EL ANSSARI A., GIL A., KORILI S.A., VICENTE M.A. Interaction of Stevensite with Cd<sup>2+</sup> and Pb<sup>2+</sup> in Aqueous Dispersions. *Applied Clay Science*, Vol. 35, No. 1-2, 2007, pp. 47-58.

- [12] ELASS K., LAACHACH A., AZZI M. Equilibrium, Thermodynamic and Kinetic Studies to Study the Sorption of Rhodamine-B by Moroccan Clay. *Global Nest Journal*, Vol. 15, No. 4, 2015, pp. 542-550.
- [13] BEJJAOUÏ R., BENHAMMOU A., NIBOU L., TANOUTI B., BONNET J.P., YAACOUBI A., AMMAR A. Synthesis and Characterization of Cordierite Ceramic from Moroccan Stevensite and Andalusite. *Applied Clay Science*, Vol. 49, No. 3, 2010, pp. 336-340.
- [14] MAMULOVÁ KUTLÁKOVÁ K., TOKARSKÝ J., KOVÁŘ P., VOJTĚŠKOVÁ S., KOVÁŘOVÁ A., SMETANA B., KUKUTSCHOVÁ J., ČAPKOVÁ P., MATĚJKA V. Preparation and Characterization of Photoactive Composite Kaolinite/TiO<sub>2</sub>. *Journal of Hazardous Materials*, Vol. 188, No. 1-3, 2011, pp. 212-220.
- [15] KOČÍ K., OBALOVÁ L., MATĚJOVÁ L., PLACHÁ D., LACNÝ Z., JIRKOVSKÝ J., ŠOLCOVÁ O. Effect of TiO<sub>2</sub> particle size on the photocatalytic reduction of CO<sub>2</sub>. *Applied Catalysis B*, Vol. 89, No. 3-4, 2009, pp. 494-502.
- [16] PTÁČEK P., FRAJKOROVÁ F., ŠOUKAL F., OPRAVIL T. Kinetics and Mechanism of Three Stages of Thermal Transformation of Kaolinite to Metakaolinite. Vol. 264, 2014, pp. 439-445.
- [17] SHVARZMAN A., KOVLER K., GRADER G.S., SHTER G.E. The Effect of Dehydroxylation/Amorphization Degree on Pozzolan Activity of Kaolinite. *Cement and Concrete Research*, Vol. 33, No. 3, 2003, pp. 405-416.
- [18] SCHERRER P. Bestimmung der Grösse und der inneren Struktur von Kolloidteilchen mittels Röntgenstrahlen. *Nachrichten von der Gesellschaft der Wissenschaften zu Göttingen, Mathematisch-Physikalische Klasse*, Vol. 26, 1918, pp. 98-100.
- [19] XU X., PANG H., ZHOU Z., FAN X., HU S., WANG Y. Preparation of Multi-Interfacial ZnO Particles and Their Growth Mechanism. *Advanced Powder Technology*, Vol. 22, No. 5, 2011, pp. 634-638.